

# Dynamics of a nearly planar domain wall with Bloch lines in a magnetic bubble film

V. P. Maslov and V. M. Chetverikov

Moscow Institute of Electrical Engineering

(Submitted 25 September 1987)

Zh. Eksp. Teor. Fiz. **94**, 270–280 (August 1988)

A system of truncated Slonczewski equations is derived to analyze the dynamics of a moving vertical Bloch line in a domain wall. It is shown that for fields parallel to the wall there is a threshold strength, below which a vertical Bloch line moves by translation, and above which  $2\pi$  Bloch lines are generated.

## INTRODUCTION

Simple finite-dimensional models for the motion of a vertical Bloch line (VBL) along a slightly curved domain wall are often used to analyze the dynamics of VBL's in uniaxial ferromagnetic magnetic bubble films with a large  $Q = K/2\pi M_s^2$ , where  $K$  is the uniaxial anisotropy constant and  $M_s$  is the spontaneous magnetization of the film.<sup>1</sup>

The purpose of the present paper is to derive a system of truncated Slonczewski equations to obtain a "point" model, in which the VBL dynamics can be described by solving a system of ordinary second-order differential equations. The complete (untruncated) system of equations treats the demagnetizing fields due to the finite film thickness and the formation of "surface magnetic charges," as well as fields whose magnitude relative to the Winter field is  $Q^{-1/2}$  (when a VBL is present) or  $Q^{-1}$  (for a pure Bloch or Néel wall). If the twisting of the azimuthal angle along the thickness of the film can be neglected, the initial system of equations can easily be simplified so that the domain wall and the azimuthal angle  $F$  depend only on time and a single spatial coordinate parallel to the wall. This "point" model is valid for weak external fields  $\lesssim 4\pi M_s (2Q)^{-1/2}$ .

Numerical solution of the truncated Slonczewski equations shows that in a strong constant external field  $H_1^0$  parallel to the wall, the solution undergoes time-periodic bifurcations which can be interpreted as corresponding to the generation of  $2\pi$  Bloch lines from an isolated moving  $\pi$  Bloch line acted on by the field  $H_1^0$ .

## 1. THE SLONCZEWSKI EQUATIONS WITH FULL ALLOWANCE FOR THE DEMAGNETIZING FIELDS

Dimensionless variables<sup>2,3</sup> will be used in this paper to simplify the formulas. The space and time scales are chosen to be the characteristic length  $l_0$  of the ferromagnet and  $T_0 = 2Q/4\pi\gamma M_s$ , respectively, where  $\gamma$  is the gyromagnetic ratio. For large  $Q$ , the maximum dimensionless Walker velocity is equal to  $1/2$ . The magnetic field is measured in units of  $4\pi M_s$ . The dimensionless (Gilbert) damping factor and the constant and characteristic angle for the orthorhombic anisotropy are equal to  $\alpha$ ,  $\varepsilon K k_p$ , and  $\varphi_p$ , respectively. The dimensionless small parameter is  $\varepsilon = (2Q)^{-1}$ . We introduce the following notation:  $\chi(x_3)$  is the characteristic function of the region  $\mathcal{D}$  occupied by the ferromagnetic film:

$$\mathcal{D} = \{x \in R^3: x_1, x_2 \in R^2, x_3 \in [0, h]\},$$

$$\chi(x_3) = \begin{cases} 1, & x \in \mathcal{D} \\ 0, & x \notin \mathcal{D} \end{cases}$$

where  $h$  is the dimensionless thickness of the film. The easy axis of the film is parallel to the vector  $\mathbf{N}_3 = \{0, 0, 1\}$ . The

isolated, nearly planar domain wall is described by the equation  $x_2 = q(t) + P(x_1, x_3, t)$ , where  $|P| \ll 1$ . The spins are assumed to point up for  $x_2 \rightarrow -\infty$  and down for  $x_2 \rightarrow \infty$ , but can vary freely on the film boundary  $\Gamma = \{x \in R^3: x_3 = 0\} \cup \{x \in R^3: x_3 = h\}$ . The boundary conditions for  $P(x_1, x_3, t)$  and for the azimuthal turning angle  $F(x_1, x_3, t)$  of the magnetization vector in the domain wall are

$$\left. \frac{\partial P}{\partial x_3} \right|_{\Gamma} = \left. \frac{\partial F}{\partial x_3} \right|_{\Gamma} = 0, \quad (1.1)$$

and the smallness of the wall curvature is expressed by

$$q \sim O(1), \quad P \sim O(\delta_0), \quad \frac{\partial P}{\partial x_{1,3}} \sim O(\delta_1), \quad \frac{\partial^2 P}{\partial x_{1,3}^2} \sim O(\delta_2), \quad (1.2)$$

where  $\delta_0, \delta_1, \delta_2 \lesssim \varepsilon^{1/2}$ . Throughout the following the symbol  $O(\varepsilon^p)$  will denote a bound with respect to the norm in the space of continuous functions, i.e., the maximum absolute value of the function for all values of its arguments.

With these notations the complete Slonczewski equations are given by

$$\alpha \frac{\partial}{\partial t} (q+P) + \varepsilon \frac{\partial F}{\partial t} - \frac{1}{2} \left( \frac{\partial^2}{\partial x_1^2} + \frac{\partial^2}{\partial x_3^2} \right) P = \mathcal{R}_1, \quad (1.3)$$

$$-\frac{\partial}{\partial t} (q+P) + \alpha \varepsilon \frac{\partial F}{\partial t} - \frac{\varepsilon}{2} \left( \frac{\partial^2}{\partial x_1^2} + \frac{\partial^2}{\partial x_3^2} \right) F$$

$$+ \frac{1}{4} k_p \sin 2(F - \varphi_p) = \mathcal{R}_2, \quad (1.4)$$

where the right-hand sides  $\mathcal{R}_1$  and  $\mathcal{R}_2$  characterize the influence of the complete magnetic field averaged over the wall thickness. This field consists of a specified external field  $\mathbf{H}^0(\mathbf{x}, t)$  and a demagnetizing field  $\mathbf{H}^d$ , which in turn is determined by the magnetostatic equations and depends in a complicated way on  $P$  and  $F$ . We will see below that  $\mathbf{H}^d$  has a decisive influence on the form of the solution of (1.3), (1.4).

The derivation of (1.3) and (1.4) is discussed in Refs. 2–4. It is based on solving the combined Landau-Lifshitz and magnetostatic equations asymptotically in the small parameter  $\varepsilon$ . Equations (1.3), (1.4) then appear as a necessary condition for the asymptotic solution to exist. Before specifying  $\mathcal{R}_1$  and  $\mathcal{R}_2$  explicitly, we give expressions for the components of the demagnetizing field that appear in them. In the context of the asymptotic expansion, each of these components may be regarded as an independent field associated with a specific magnetic charge distribution on the film and domain wall.

Using the notation

$$\mathbf{x}_\perp = \{x_1, 0, x_3\}, \quad \mathbf{k}_\perp = \{k_1, 0, k_3\}, \quad k = |\mathbf{k}_\perp|,$$

$$\begin{pmatrix} f_1(\mathbf{x}_\perp) \\ f_2(\mathbf{x}_\perp) \\ f_3(\mathbf{x}_\perp) \end{pmatrix} = \begin{pmatrix} \sin F - \cos F \frac{\partial P}{\partial x_1} \\ \chi(r_3) \varepsilon \frac{\partial}{\partial x_1} \cos F \\ \chi(r_3) \frac{\partial P}{\partial x_3} \end{pmatrix} = \int \frac{dk_1 dk_3}{(2\pi)^2} \exp[i(\mathbf{k}_\perp, \mathbf{x}_\perp)] \begin{pmatrix} \tilde{f}_1(\mathbf{k}_\perp) \\ \tilde{f}_2(\mathbf{k}_\perp) \\ \tilde{f}_3(\mathbf{k}_\perp) \end{pmatrix}, \quad (1.5)$$

$$\sigma(\varepsilon k) = \frac{2}{\pi} \sum_{n=0}^{\infty} \frac{(-1)^n}{n+1/2+\varepsilon k/2},$$

we have the following expressions for the various fields:

0) The Winter field is

$$\{0, -\sin F \sin G, 0\}, \quad \text{where } G = 2 \operatorname{arctg} \exp[(x_2 - q - P)\varepsilon^{-1}]. \quad (1.6)$$

This is the principal term in the  $\varepsilon$ -expansion of the local demagnetizing field.

1) The long-range field  $\mathbf{H}^{(1)}$ , collinear with the Winter field, is of the form

$$\mathbf{H}^{(1)} = \{0, H_2^{(1)}, 0\},$$

$$H_2^{(1)} = \int \frac{dk_1 dk_3}{(2\pi)^2} \exp[i(\mathbf{k}_\perp, \mathbf{x}_\perp)] \tilde{f}_1(\mathbf{k}_\perp) \varepsilon k \sigma(\varepsilon k) \cdot \exp[-k|x_2 - q - P|]. \quad (1.7)$$

It describes the nonlocal part of the field  $\mathbf{H}^d$  due to spatial variations in the distribution of the  $\pi$ -charges along the surface of the wall.

2) The local field along the wall is

$$-\varepsilon(G - \pi/2) \nabla_\perp f_1(\mathbf{x}_\perp). \quad (1.8)$$

It also stems from the nonuniform distribution of  $\pi$ -charges along the wall.

3) The Coulomb field

$$\mathbf{H}^{(3)} = \frac{\pi}{2} \int \frac{dk_1 dk_3}{(2\pi)^2} \exp[i(\mathbf{k}_\perp, \mathbf{x}_\perp)] \tilde{f}_2(\mathbf{k}_\perp) \frac{i\mathbf{k}_\perp}{k} \sigma(\varepsilon k) \cdot \exp[-k|x_2 - q - P|] \quad (1.9)$$

is directed along the wall and is present due to the nonuniformity of the  $\sigma$ -charge distribution along the domain wall;

4) The field

$$\mathbf{H}^{(4)} = \int \frac{dk_1 dk_3}{(2\pi)^2} \exp[i(\mathbf{k}_\perp, \mathbf{x}_\perp)] \tilde{f}_3(\mathbf{k}_\perp) \frac{i\mathbf{k}_\perp}{k} \exp[-k|x_2 - q - P|] \quad (1.10)$$

associated with the transverse bending of the domain wall is also parallel to the wall. It is due to the presence of an effective charge on the surface of the curved wall.

5) The field associated with the surface charge distribution is expressible as a sum of local and nonlocal fields,

$$\mathbf{H}^{(5)} = \mathbf{H}^{(5l)} + \mathbf{H}^{(5nl)}. \quad (1.11)$$

Its source is the effective magnetic charge on the surface  $\Gamma$ .

Outside an  $\varepsilon$ -neighborhood of the intersection of the domain wall with the film surface, the expressions for the

local components of the fields are

$$H_1^{(5l)} = -\frac{1}{\pi} \{P'(x_1, 0, t) \ln[(x_2 - q)^2 + x_3^2]^{1/2} - P'(x_1, h, t) \ln[(x_2 - q)^2 + (h - x_3)^2]^{1/2}\},$$

$$H_2^{(5l)} = -\frac{1}{2\pi} \ln \frac{(h - x_3)^2 + (x_2 - q - P)^2}{x_3^2 + (x_2 - q - P)^2}, \quad (1.12)$$

$$H_3^{(5l)} = \frac{1}{\pi} \left( \operatorname{arctg} \frac{x_2 - q - P}{h - x_3} + \operatorname{arctg} \frac{x_2 - q - P}{x_3} \right).$$

Similarly, for the nonlocal field components we have the expressions

$$\mathbf{H}^{(5nl)} = -\nabla I^{(5nl)}, \quad (1.13)$$

$$I^{(5nl)} = \frac{1}{\pi} \int \frac{d\kappa}{2\pi} e^{i\kappa x_1} \{ \mathcal{P}(\kappa, h, t) \cdot [K_0(|\kappa| [(x_2 - q)^2 + (h - x_3)^2]^{1/2}) + \ln((x_2 - q)^2 + (h - x_3)^2)^{1/2}] - \mathcal{P}(\kappa, 0, t) [K_0(|\kappa| [(x_2 - q)^2 + x_3^2]^{1/2}) + \ln((x_2 - q)^2 + x_3^2)^{1/2}] \},$$

where  $K_0(z)$  is the modified Bessel function of the second kind:

$$K_0(z) = \int_0^{\infty} d\xi \exp(-z \operatorname{ch} \xi),$$

$$P(x_1, x_3, t) = \int \frac{d\kappa}{2\pi} e^{i\kappa x_1} \mathcal{P}(\kappa, x_3, t).$$

Near the intersection of the domain wall with the film surface, the leading term in the asymptotic expansion of (1.11) is obtained by multiplying (1.12), (1.13) by the function  $(2\varepsilon)^{-1} \cosh^{-2}[(x_2 - x_2')/\varepsilon]$  and integrating over  $x_2'$ .

Once all the components of the demagnetizing field (1.6)–(1.11) have been determined, the right-hand sides of the Slonczewski equations (1.3), (1.4) can be expressed in the form<sup>2-4</sup>

$$\mathcal{A}_1 = (\mathbf{H}^0 + \mathbf{H}^{(3)} + \mathbf{H}^{(4)} + \mathbf{H}^{(5)}, N_s) |_{x_2=q+P} + \frac{\varepsilon}{2} \frac{\partial}{\partial x_1} \sin 2F + O(\varepsilon), \quad (1.14)$$

$$\mathcal{A}_2 = -\frac{1}{2} \sin 2F$$

$$\begin{aligned}
& + \frac{1}{2} \int_{-\infty}^{\infty} \frac{dx_2}{\varepsilon} (\mathbf{H}^0 + \mathbf{H}^{(1)} + \mathbf{H}^{(3)} + \mathbf{H}^{(4)} + \mathbf{H}^{(5)}, \mathbf{N}_2) \sin G \\
& + \frac{\partial P}{\partial x_1} \cos 2F, \quad (1.15)
\end{aligned}$$

where

$$\mathbf{N}_2 = \{-\sin F, \cos F, 0\}.$$

The first term in  $\mathcal{R}_2$  describes the effects of the Winter field, while the local field along the wall (1.8) is accounted for by the last terms in  $\mathcal{R}_1$  and  $\mathcal{R}_2$ . The origin of the remaining terms in (1.14), (1.15) is clear from Eqs. (1.7), (1.9)–(1.11).

The self-consistent description of the dynamics of a nearly planar domain wall containing a Bloch line in a magnetic bubble film thus reduces to solving two integro-differential equations in a region, with the boundary conditions (1.1), for two scalar functions:  $q(t) + P(x_1, x_3, t)$  and  $F(x_1, x_3, t)$ . The latter determine the position and the structure of the domain wall, respectively.

Because of the great difficulty in analyzing the full system of Slonczewski equations, to obtain specific results we are forced to make further simplifications. In this paper we consider the situation when the dependence of  $P$  and  $F$  on the spatial coordinate  $x_3$  can be neglected on physical grounds.

## 2. TRUNCATED SLONCZEWSKI EQUATIONS

We express the external field  $\mathbf{H}^0(\mathbf{x}, t)$  as the sum of a spatially uniform field  $\mathbf{H}^0(t)$  and a quadrupole field

$$\mathbf{H}^q = \{0, -(x_3 - h/2)H', -x_2H'\}, \quad H' = \text{const.}$$

The latter is known to stabilize the domain wall,<sup>5,6</sup> and in addition we can choose  $H'$  so as to make the field  $H_2^{(5)} + H_2^q$  small even in an  $\varepsilon$ -neighborhood of the intersection of the domain wall with the film boundary  $\Gamma$ . To first order, we therefore need not consider the twisting of the wall.<sup>7,8</sup> If  $\partial F/\partial x_3 \sim O(\varepsilon)$  and  $\partial P/\partial x_3 \sim O(\varepsilon)$ , then the Slonczewski equations (1.3), (1.4), averaged over the thickness of the film, depend only on a single spatial variable  $x_1$ :

$$\begin{aligned}
\alpha \frac{\partial}{\partial t} (q + P) + \varepsilon \frac{\partial F}{\partial t} &= \frac{1}{2} \frac{\partial^2}{\partial x_1^2} P + H_3^0(t) - (q + P)H' \\
& - \varepsilon \frac{\partial F}{\partial x_1} \cos 2F + \overline{H_3^{(5)}}, \quad (2.1) \\
-\frac{\partial}{\partial t} (q + P) + \alpha \varepsilon \frac{\partial F}{\partial t} &= \frac{\varepsilon}{2} \frac{\partial^2}{\partial x_1^2} F - \frac{1}{2} \sin 2F \\
& - \frac{1}{4} k_p \sin 2(F - \varphi_p) + \frac{\partial P}{\partial x_1} \cos 2F \\
& - \frac{\pi}{2} \{ (H_1^0 + \overline{H_1^{(3)}}) \sin F - (H_2^0 + \overline{H_2^{(1)}}) \cos F \}, \quad (2.2)
\end{aligned}$$

where the overbars and angle brackets indicate averages over the thickness of the film and wall, respectively:

$$\begin{aligned}
\overline{H_3^{(5)}} &= -\frac{1}{h} \int_0^h dx_3 \frac{\partial}{\partial x_3} I^{(5)}(x_1, x_2 = q, x_3, t) \\
&= \frac{1}{\pi^2 h} \int_{-\infty}^{\infty} dx e^{ix_1} \overline{P}(\mathbf{x}, t) \left[ C_E + K_0(|\mathbf{x}|h) + \ln \frac{|\mathbf{x}|h}{2} \right], \quad (2.3)
\end{aligned}$$

$$\overline{P}(\mathbf{x}, t) = \int dx_1 P(x_1, t) e^{-ix_1},$$

where  $C_E = 0.5772\dots$  is Euler's constant,

$$\begin{aligned}
\overline{H_1^{(3)}} &= \frac{1}{2} \int d\xi \left[ \varepsilon \frac{\partial}{\partial \xi} \cos F(\xi, t) \right] (x - \xi)^{-1} h^{-1} \\
& \cdot \{ [(x - \xi)^2 + h^2]^{1/2} - |x - \xi| \}, \quad (2.4)
\end{aligned}$$

$$\overline{H_2^{(1)}} = \frac{\pi}{2} \int \frac{dk_1}{2\pi} e^{ik_1 x_1} \overline{f}_1(k_1) \varepsilon |k_1| \sigma^2(\varepsilon |k_1|), \quad (2.5)$$

$$\overline{f}_1(k_1) = \int dx_1 e^{-ih_1 x_1} \left( \sin F - \frac{\partial P}{\partial x_1} \cos F \right).$$

The contribution from the component (1.10) of the demagnetizing field to  $\mathcal{R}_1$  and  $\mathcal{R}_2$  disappears after averaging over the thickness of the film.

It can be shown that if  $H_3^0(x, t) \sim O(1)$  and  $H_1^0 \sim H_2^0 \sim O(\varepsilon^{1/2})$ , then Eq. (2.1) is correct to within  $O(\varepsilon^{3/2})$ , while (2.2) holds to within  $O(\varepsilon)$ . If on the other hand we assume that  $H_2^{(5)} + H_2^q \sim O(\varepsilon^{1/2})$ , then Eqs. (2.1) and (2.2) both have the same error  $O(\varepsilon^{3/2})$ . The equations (2.1), (2.2) admit several types of solutions which describe small flexural oscillations of the Bloch wall as well as complex motions involving several vertical Bloch lines.

In this paper we will treat only the following two problems in detail.

1. Find the behavior of an isolated VBL in a nearly planar domain wall in a ferromagnet with weak rhombic anisotropy ( $k_p \lesssim \varepsilon^{1/2}$ ) in fields  $|\mathbf{H}^0| \lesssim \varepsilon^{1/2}$  for  $H' \sim 1$ .

2. Study the generation of VBL pairs from a single moving VBL.

## 3. DYNAMICS OF AN ISOLATED VERTICAL BLOCH LINE

We will henceforth omit the subscript 1 in the spatial variables and write simply  $x$  for  $x_1$ .

To make the formulas more compact, we first introduce some auxiliary functions  $q_i(t)$ ,  $F_0(x; t)$ ,  $P_0(x; t)$ ,  $R(x, t)$ , and  $X(t)$ . We define  $F_0(x; t)$  and  $P_0(x; t)$  by

$$F_0(x; t) = 2 \arctg \exp \left\{ \left( \frac{2}{\varepsilon} \right)^{1/2} [x - X(t)] \right\}, \quad (3.1)$$

$$\begin{aligned}
P_0(x; t) &= 2^{1/2} \varepsilon^{1/2} \sin F_0 - (2H')^{1/2} \varepsilon^2 \\
& \cdot \sum_{n=0}^{\infty} (-1)^n \left[ \left( n + \frac{1}{2} \right)^2 - \frac{H' \varepsilon}{4} \right]^{-1} \\
& \cdot \left\{ \left( n + \frac{1}{2} \right) \exp[-(2H')^{1/2} |x - X(t)|] \right. \\
& \left. - \left( \frac{H' \varepsilon}{4} \right)^{1/2} \exp \left[ -2 \left( n + \frac{1}{2} \right) \left( \frac{2}{\varepsilon} \right)^{1/2} |x - X(t)| \right] \right\}, \quad (3.2)
\end{aligned}$$

while  $q_i(t)$ ,  $R(x, t)$ , and  $X(t)$  satisfy the equations

$$\begin{aligned}
\ddot{q}_1 + \alpha \dot{q}_1 + H' q_1 &= H_3^0(t), \quad (3.3) \\
\left( \alpha \frac{\partial}{\partial t} + \varepsilon^2 \frac{\partial^2}{\partial t^2} - \frac{1}{2} \frac{\partial^2}{\partial x^2} + H' \right) R \\
& - \int \frac{d\mathbf{x}}{\pi^2 h} e^{i\mathbf{x} \cdot \mathbf{x}} \left[ C_E + K_0(|\mathbf{x}|h) \right. \\
& \left. + \ln \frac{|\mathbf{x}|h}{2} \right] \overline{R}(\mathbf{x}, t) = \dot{X} \left( \frac{2}{\varepsilon} \right)^{1/2} \left[ \sin F_0 - \frac{\pi}{2} (H_2^0 \right.
\end{aligned}$$

$$\begin{aligned}
& + \langle \overline{H_2^{(1)}} \rangle \sin^2 F_0 \\
& + \frac{1}{4} k_p \cos \varphi_p \sin F_0 + \frac{1}{4} (2\varepsilon)^{-1/2} [x - X(t)] \cos \varphi_p \sin 2F_0,
\end{aligned} \quad (3.4)$$

$$\begin{aligned}
& \dot{q}_1 \pi [1 + 4/3 (H_2^0 + \langle \overline{H_2^{(1)}} \rangle) |_{x=X} - 1/6 k_p \cos \varphi_p] + \alpha \varepsilon \pi \dot{q} \\
& - \pi (H_1^0 + \langle \overline{H_1^{(3)}} \rangle) |_{x=X} - 2^{3/2} \alpha \varepsilon^{1/2} \dot{X} [1 - 1/2 \pi (H_2^0 \\
& \quad + \langle \overline{H_2^{(1)}} \rangle) |_{x=X} \\
& + 1/8 k_p \cos \varphi_p] - 1/3 \pi k_p (H_2^0 + \langle \overline{H_2^{(1)}} \rangle) |_{x=X} \sin \varphi_p \\
& + 1/3 \pi (k_p/4)^2 \sin 2\varphi_p \\
& = \varepsilon \int \frac{\partial R}{\partial x} \cos 2F_0 dF_0 - 2\varepsilon \int \frac{\partial R}{\partial t} \sin^2 F_0 dF_0.
\end{aligned} \quad (3.5)$$

It can be shown that the functions

$$q + P = q_1(t) + P_0(x; t) + \varepsilon R(x, t) + O(\varepsilon^2), \quad (3.6)$$

$$\begin{aligned}
F = F_0(x; t) + \dot{q}_1(t) + \varepsilon \partial R / \partial t + 1/2 \pi (H_2^0 + \langle \overline{H_2^{(1)}} \rangle) \cos F_0 \\
- 1/4 k_p \sin \varphi_p + 1/4 k_p \cos \varphi_p (2/\varepsilon)^{1/2} [x - X(t)] \sin F_0 + \varepsilon f
\end{aligned} \quad (3.7)$$

satisfy the system (2.1), (2.2) to within terms  $O(\varepsilon^{3/2})$ . The function  $q_1(t)$  describes the spatially uniform motion of a domain wall subject to the bias field  $H_3^0(t)$ . The functions  $P_0(x; t)$  and  $\varepsilon R(x, t)$  respectively characterize the static and dynamic bending of a domain wall with a VBL, and  $X(t)$  gives the position of the VBL along the wall.

The static bending of the domain wall in the vicinity of the VBL is due to the component (1.8) of the demagnetizing field, which appears in  $\mathcal{R}_1$  and  $\mathcal{R}_2$  locally through the first spatial derivatives  $\partial F / \partial x_1$  and  $\partial P / \partial x_1$ .

The averaged fields appearing in (3.4) and (3.5) have the form

$$\begin{aligned}
\langle \overline{H_2^{(1)}} \rangle = -\pi \left( \frac{\varepsilon}{2} \right)^{1/2} \left\{ \text{ch}^{-2} z - (2\pi^2)^{-1} \left[ \psi' \left( \frac{1}{4} + iz_1 \right) \right. \right. \\
\left. \left. + \psi' \left( \frac{1}{4} - iz_1 \right) \right] \right\} + O(\varepsilon),
\end{aligned} \quad (3.8)$$

$$\begin{aligned}
\langle \overline{H_1^{(3)}} \rangle = \left( \frac{\varepsilon}{2} \right)^{1/2} \int_{-\infty}^{\infty} d\xi \text{ch}^{-2} \left\{ \left( \frac{2}{\varepsilon} \right)^{1/2} [\xi - X(t)] \right\} \\
\times (x - \xi)^{-1} \frac{|h^2 + (x - \xi)^2|^{1/2} - |x - \xi|}{h} + O(\varepsilon),
\end{aligned}$$

where

$$z = (2/\varepsilon)^{1/2} [x - X(t)], \quad z_1 = z/2\pi,$$

$$\psi'(\xi) = \frac{d^2}{d\xi^2} \ln \Gamma(\xi) = \sum_{n=0}^{\infty} (\xi + n)^{-2},$$

$\Gamma(\xi)$  is the gamma-function. This result can be proved by substituting (3.6), (3.7) into (2.1), (2.2) and estimating the remaining terms. Equation (3.5) is a necessary condition for the existence of the correction  $\varepsilon f$  in Eq. (3.7).

The region of validity of Eqs. (3.4), (3.5) can be found more precisely by comparing them with Eqs. (11)–(13) in Refs. 9, 10. To do this a further simplification is necessary, in which we neglect all but the leading terms in  $\varepsilon$  in (3.4), (3.5).

We begin with Eq. (3.4). The integral term on the left in (3.4) is just the field  $\varepsilon^{-1} \overline{H_3^{(5\pi l)}}$  produced by the dynamic bending of the domain wall. For small  $H'$ , it leads to flexural instability of the wall.<sup>5,6</sup> However, for values  $H' > 0$  such that

$$\begin{aligned}
& \frac{(kh)^2}{2} + H'h^2 \\
& - \frac{2h}{\pi} \left[ C_{E+K_0}(|k|h) + \ln \frac{|k|h}{2} \right] > 0
\end{aligned} \quad (3.9)$$

holds for all  $k \in R^1$ , the field  $\overline{H_3^{(5\pi l)}}$  can be neglected, as we will see below that its magnitude is actually  $\sim O(\varepsilon)$ . Numerical analysis of the condition (3.9) reveals that for a fixed  $h$ , it holds for  $H' > H'_{\min}$ . If  $H' = H'_{\min}$ , the left-hand side of (3.9) vanishes at the single point  $|k| = \kappa_{\min}$ . Figure 1 shows how  $H'_{\min}$  and  $\kappa_{\min}$  depend on the thickness  $h$  of the film.

Retaining only the leading terms in  $\varepsilon$  in (3.4), we obtain a much simpler equation for the dynamic wall bending,

$$\left( \alpha \frac{\partial}{\partial t} - \frac{1}{2} \frac{\partial^2}{\partial x^2} + H' \right) R = \dot{X}(t) \left( \frac{2}{\varepsilon} \right)^{1/2} \sin F_0. \quad (3.10)$$

Similarly, if we discard all but the leading terms in  $\varepsilon$  in (3.5), we obtain the following integro-differential equation for the position of the VBL:

$$\begin{aligned}
& 2\varepsilon^{1/2} \left( 2^{1/2} \alpha \dot{X} - \frac{\pi}{2} \varepsilon^{-1/2} H_1^0 \right) + \pi \dot{q}_1 \\
& + \varepsilon \int_{-\infty}^{\infty} dx \frac{\partial F_0}{\partial x} \left( \frac{\partial R}{\partial t} 2 \sin^2 F_0 - \frac{\partial R}{\partial x} \cos 2F_0 \right) = 0.
\end{aligned} \quad (3.11)$$

Equations (3.10) and (3.11) can be obtained from the initial equations (2.1), (2.2) by keeping only the terms through order  $O(\varepsilon)$ .<sup>11</sup> We will confine ourselves to this approximation in what follows, so that our starting point is the system of the three equations (3.3), (3.10), (3.11). Using (3.3), it is easy to show that the velocity of the domain wall as a whole is  $\dot{q}_1 \sim O(\varepsilon^{1/2} \alpha^{-1})$ . The static bending  $P_0(x; t)$  of a wall with an isolated VBL is due to the correction (1.8), of order  $\varepsilon^{1/2}$ , to the local Winter demagnetizing field, and

$$\max_x P_0(x; t) \sim O(\varepsilon^{1/2}), \quad \int_x P_0 dx = 0, \quad \int |P_0| dx \sim O(\varepsilon^2). \quad (3.12)$$

The dynamic twisting of a domain wall with a moving VBL is given by  $\varepsilon R(x, t)$ , and we have the estimates

$$|R(x, t)| \leq \text{const} \cdot \max_t |X(t)| (H')^{-1/2}, \quad (3.13)$$

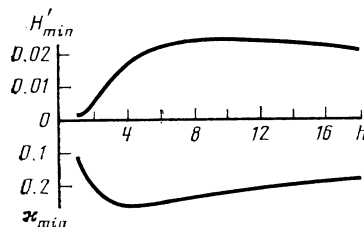


FIG. 1. Dependence of  $H'_{\min}$  and  $\kappa_{\min}$  on film thickness.

$$\int R(x, t) dx = \frac{\pi}{\alpha} \int_0^t d\nu \dot{X}(\nu) \exp\left[-\frac{H'}{\alpha}(t-\nu)\right].$$

Equations (3.12) and (3.13) show first that the dynamic bending of the wall is roughly  $\varepsilon^{-1/2}$  times greater than the static bending, and second that Nikiforov and Sonin<sup>10</sup> were correct in suggesting that the spatial scale of the bending caused by the motion of the VBL is much greater than the width of the VBL.

Like the orthorhombic anisotropy in the above approximation, the long-range fields  $\langle H_1^{(3)} \rangle$  and  $\langle H_2^{(1)} \rangle$  do not contribute to the VBL dynamics, owing to the symmetry in Eqs. (3.8); they significantly affect only the distribution of the azimuthal angle  $F$  along the wall.

We now discuss Eq. (3.11), which describes the dynamics of the VBL. It can be simplified substantially for small and large times by using asymptotic formulas for the dynamic bending  $R(x, t)$ . For  $t \ll \varepsilon\alpha$ ,

$$R(x, t) \approx \alpha^{-1} \left(\frac{2}{\varepsilon}\right)^{1/2} [X(t) - X(0)] / \text{ch}\left\{\left(\frac{2}{\varepsilon}\right)^{1/2} [x - X(t)]\right\} \quad (3.14)$$

so that the principal term in the integral in (3.11) is equal to  $2^{3/2}\varepsilon^{1/2}\alpha^{-1}\dot{X}$ . The VBL thus moves without inertia at small times (we have a first-order equation), and the onset of dynamic bending effectively amounts to a renormalization of the damping factor, with  $\alpha$  replaced by  $\alpha + \alpha^{-1}$ . If the functions  $\dot{q}_1(t)$  and  $H_1^{(0)}(t)$  are both constant for  $t \gg \alpha/H'$ , then the velocity  $\dot{X}$  of the VBL is constant and satisfies

$$2^{1/2}\alpha\dot{X} - \pi\varepsilon^{-1/2}H_1^0 + \pi\varepsilon^{-1/2}\dot{q}_1 + \pi^2\alpha[e/(2H' + \alpha^2\dot{X}^2)]^{1/2}\dot{X}^3 = 0, \quad (3.15)$$

and the dynamic bending is given by the expression

$$R(x, t) = \varepsilon^{1/2}\dot{X} \int dy \frac{\cos[y(x-X)\varepsilon^{-1/2}]}{\text{ch}(2^{1/2}\pi y)} \frac{y^2 + 2\varepsilon H'}{(y^2 + 2\varepsilon H')^2 + 4y^2\varepsilon\alpha\dot{X}^2} - 2\varepsilon\alpha\dot{X}^2 \int dy \frac{\sin[y(x-X)\varepsilon^{-1/2}]}{\text{ch}(2^{1/2}\pi y)} \frac{y}{(y^2 + 2\varepsilon H')^2 + 4y^2\varepsilon\alpha\dot{X}^2}. \quad (3.16)$$

The first two terms in (3.15) have an obvious physical interpretation; they correspond to inertialess VBL motion in the field  $H_1^0$ , which acts to increase the size of an energetically favorable subdomain. The third term accounts for the gyroscopic pressure on the Bloch line exerted by a planar domain wall moving as a whole. The fourth term describes the dissipative nonlinearity caused by the gyroscopic pressure on the Bloch line (averaged over the width of the line) exerted by the moving curved region of the domain wall, the curvature itself being determined by the VBL dynamics.

It is clear from Eq. (3.16) that for a uniformly moving VBL, the bending is not symmetric in the variable  $x - X(t)$ , the asymmetry being proportional to the damping constant  $\alpha$ . The stage of nonuniform VBL motion is more complicated, and the reduction of the integro-differential equation (3.11) to a second-order dynamic equation, as was done in Ref. 12, requires further assumptions regarding the orders of magnitude of the higher time-derivatives of  $X(t)$ . If it is legitimate to neglect all the derivatives of order higher than two then the term linear in  $\ddot{X}$ , which serves as a correction on the

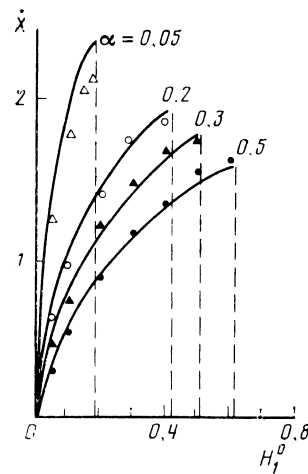


FIG. 2. Steady-state VBL velocity versus field  $H_1^0$  in the plane of the wall for several different damping factors  $\alpha$ . The points give values obtained by solving the Slonczewski equations numerically; the solid curves give the results of the point model (3.15); the dashed curves show the onset of generation of  $2\pi$  Bloch lines.

left-hand side of the steady-state equation (3.15), will have the form

$$\pi^2\varepsilon^{1/2}[(2H')^{-1/2} + O(\alpha^2\dot{X}^2/H')] \dot{X}. \quad (3.17)$$

Formally, the term (3.17) appears in (3.15) because of the time dependence of the averaged gyroscopic pressure exerted on the Bloch line by a bend in the wall moving with a nonuniform velocity. The form of the term (3.17) permits us to introduce an effective VBL mass, for which a physical interpretation was suggested in Refs. 9, 10.

To within the above approximation, Eq. (3.15) with the inertial term (3.17) coincides with the Zvezdin-Popkov equation.<sup>12</sup> A derivation of this equation for  $H_1^0 \sim \alpha$ ,  $0 < \alpha \ll 1$ , is given in Refs. 13 and 14. Note that we have taken  $\varepsilon^{1/2}$  as the small parameter in Sec. 3, so that we are implicitly assuming that  $\varepsilon^{1/2} \ll \alpha < 1$ . The fact that the same equation for the VBL dynamics was obtained in Refs. 13, 14 with  $\alpha$  as the formal small parameter (for starting equations simpler than the system (2.1), (2.2)) indicates that the result is also valid for  $0 < \alpha \lesssim \varepsilon^{1/2}$  when  $|H_1^0| \lesssim \alpha$ . In other words, Eqs. (3.15) and (3.17) correctly describe the VBL dynamics for arbitrary ratios  $\alpha/\varepsilon^{1/2}$  and fields  $|H_1^0| \lesssim \min(\alpha, \varepsilon^{1/2})$ . Numerical calculations<sup>11</sup> show that the steady-state result (3.15) agrees closely with the solution of the starting system (2.1), (2.2). Figure 2 shows how the velocity of the vertical Bloch line depends on the external field  $H_1^0$  for  $\varepsilon = 0.1$ ,  $H' = 1$ ,  $H_2^0 = 0$ ,  $H_3^0 = 0$ , and  $k_p = 0$  for several values of  $\alpha$ . In these results we have neglected the fields  $\overline{H_3^{(5n)}}$ ,  $\langle H_1^{(3)} \rangle$ , and  $\langle H_2^{(1)} \rangle$  in (2.1), (2.2). The solid curves show the steady-state VBL velocities calculated from (3.15) as a function of the field  $H_1^0$ , and the points show the results obtained by numerically solving the Cauchy problem for the system (2.1), (2.2) with the boundary conditions

$$\frac{\partial P}{\partial x} \rightarrow 0, \quad |x| \rightarrow \infty; \quad \frac{\partial F}{\partial x} \rightarrow 0, \quad |x| \rightarrow \infty$$

and with initial distributions  $P$  and  $F$  corresponding to an isolated VBL at rest.

According to Fig. 2, Eq. (3.15) closely approximates

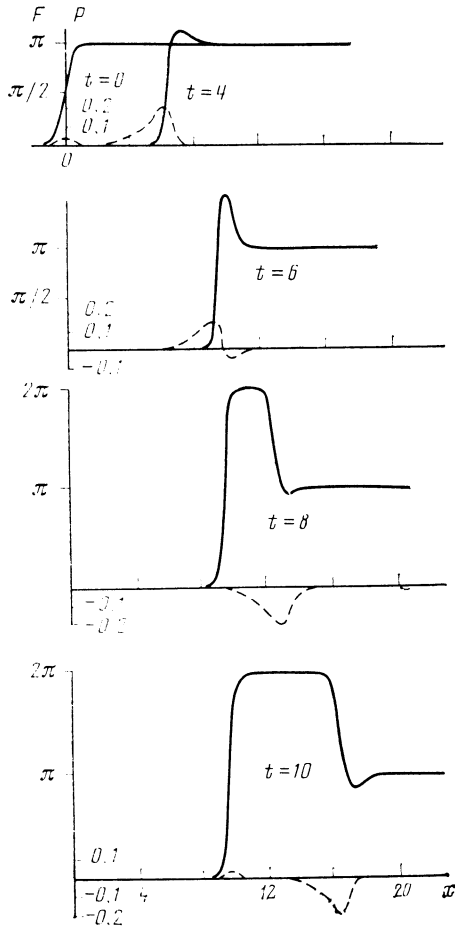


FIG. 3. Time evolution of the generation of  $2\pi$  Bloch lines in a field directed in the plane of the wall. The solid and dashed curves show  $F$  and  $P$ , respectively.

the steady-state velocity of a VBL for a wider range of parameter values than was assumed in the derivation. Numerical investigation of the above Cauchy problem is thus necessary in order to determine the range of  $\alpha$  and  $H_1^0$  values beyond which Eq. (3.15) for steady VBL motion deviate substantially from the results found by solving the truncated system of Slonczewski equations (2.1), (2.2).

We note that for all the values  $10^{-2} \leq \alpha \leq 0.5$  and  $10^{-1} \leq H' \leq 2.5$  investigated, there exist in-plane fields  $H_1^0 > 0$  above which the notion of an isolated VBL becomes meaningless due to the onset of generation of  $2\pi$  Bloch lines. A typical sequence by which this happens is shown in Fig. 3 ( $\varepsilon = 0.1$ ,  $\alpha = 0.5$ ,  $H' = 1$ ,  $H_2^0 = H_3^0 = k_p = 0$ ). This pro-

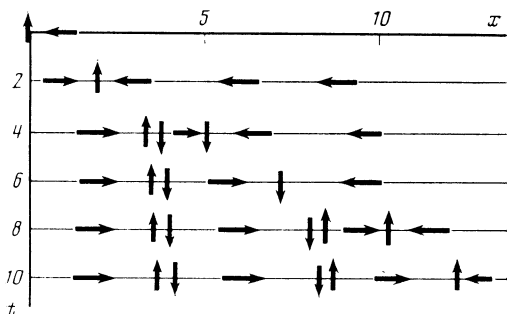


FIG. 4. Schematic diagram showing a quasistatic VBL lattice. The arrows show the direction of the magnetization in the domain wall.

cess is repeated at later times, and the newly generated  $2\pi$  Bloch lines form a quasistatic lattice (Fig. 4), in the sense that its parameters change too slowly to be detectable within our numerical accuracy. An isolated  $2\pi$  Bloch line is a static solution of the system (2.1), (2.2) when a field  $H_1^0$  is present; Fig. 3 therefore illustrates how the motion of the VBL is accompanied by a transition of the distribution  $F$  from a stable state with  $H_1^0 = 0$  to a stable state with nonzero  $H_1^0$ . This transition is driven by the gyrotropic force.

We also see from Fig. 2 that the region of validity of Eq. (3.15) is further restricted by the requirement that the damping coefficient  $\alpha$  be small ( $\leq 0.05$ ) for fields which are reasonably large ( $H_1^0 \gg \alpha$ ) but below the threshold for generation of  $2\pi$  lines.

Our numerical experiment, starting with an isolated vertical Bloch line, does not give the characteristic cluster distribution described in Refs. 13–15, where solutions of the truncated Slonczewski equations were considered without damping or an external field. Those solutions were self-similar, the  $x$  and  $t$  variables occurring only in the form  $x - ut$ . The velocity  $u$  of the VBL was a free parameter, whereas in our case it is determined by the external field  $H_1^0$  and the dissipation. It is possible, as suggested by A. F. Popkov, that a stable self-similar cluster with  $H_1^0 \neq 0$  and  $\alpha \neq 0$  might be detected numerically by choosing a more complicated initial angular distribution  $F$ . However, this conjecture requires verification.

We observe in closing that to discuss actual physical experiments, one must also estimate how the dynamics of a horizontal Bloch line affects the behavior of a VBL when  $H_1^0 \neq 0$ . However, this would require that we consider a more complicated problem involving two spatial dimensions and no averaging over the thickness of the film, which lies beyond the scope of this paper.

<sup>1)</sup>The calculations were carried out by E. E. Kotova, a student at the Moscow Institute of Electrical Engineering.

<sup>1A)</sup>A. P. Malozemoff and J. G. Slonczewski, *Magnetic Domain Walls in Bubble Materials*, *Appl. Solid State Sci., Suppl. 1*, Academic Press, New York (1979).

<sup>2)</sup>V. P. Maslov and V. M. Chetverikov, *Teor. Mat. Fiz.* **60**, 447 (1984).

<sup>3)</sup>V. P. Maslov and V. M. Chetverikov, *Dokl. Akad. Nauk* **287**, 821 (1986) [*Sov. Phys. Dokl.* **31**(4), 303 (1986)].

<sup>4)</sup>V. P. Maslov and V. M. Chetverikov, *Teoriya Domennykh Struktur v Magnitnykh Plenkakh c Bol'shoi Perpendikulyarnoĭ Anisotropiei (Theory of Domain Structures with a Large Perpendicular Anisotropy)*, Izd. VINITI, Moscow (1986).

<sup>5)</sup>F. B. Hagedorn, *J. Appl. Phys.* **41**, 1161 (1970).

<sup>6)</sup>E. Schlömann, *IEEE Trans. Magn.* **10**, 11 (1974).

<sup>7)</sup>V. G. Bar'yakhtar and B. A. Ivanov, *V Mire Magnitnykh Domenov (The World of Magnetic Domains)*, Naukova Dumka, Kiev (1986).

<sup>8)</sup>T. H. O'Dell, *Ferromagnetodynamics: The Dynamics of Magnetic Bubbles, Domains, and Domain Walls*, Wiley, New York (1981).

<sup>9)</sup>A. V. Nikiforov and É. B. Sonin, *Pis'ma Zh. Eksp. Teor. Fiz.* **40**, 325 (1984) [*JETP Lett.* **40**, 1119 (1984)].

<sup>10)</sup>A. V. Nikiforov and É. B. Sonin, *Zh. Eksp. Teor. Fiz.* **90**, 1309 (1986) [*Sov. Phys. JETP* **63**, 766 (1986)].

<sup>11)</sup>V. M. Chetverikov, in: *Proc. Tenth All-Union Sem. on New Magnetic Materials in Microelectronics, Part II*, Riga (1986), p. 231.

<sup>12)</sup>A. K. Zvezdin and A. F. Popkov, *Pis'ma Zh. Eksp. Teor. Fiz.* **41**, 90 (1985) [*JETP Lett.* **41**, 107 (1985)].

<sup>13)</sup>A. K. Zvezdin and A. F. Popkov, *Zh. Eksp. Teor. Fiz.* **91**, 1789 (1986) [*Sov. Phys. JETP* **64**, 1059 (1986)].

<sup>14)</sup>N. E. Kulagin and A. F. Popkov, *Fiz. Met. Metalloved.* **63**, 428 (1987).

<sup>15)</sup>N. E. Kulagin and A. F. Popkov, *Pis'ma Zh. Eksp. Teor. Fiz.* **43**, 197 (1986) [*JETP Lett.* **43**, 249 (1986)].

Translated by A. Mason